THE JOURNAL OF PHYSICAL CHEMISTRY Letters

Letter

pubs.acs.org/JPCL

Noncanonical Photocycle Initiation Dynamics of the Photoactive Yellow Protein (PYP) Domain of the PYP-Phytochrome-Related (Ppr) Photoreceptor

L. Tyler Mix,[†] Miwa Hara,[‡] Rachana Rathod,[‡] Masato Kumauchi,[‡,§] Wouter D. Hoff,[‡] and Delmar S. Larsen*[,†]

[†]Department of Chemistry, University of California, Davis, One Shields Avenue, Davis, California 95616, United States

[‡]Department of Microbiology and Molecular Genetics, Oklahoma State University, Stillwater, Oklahoma 74078, United States

Supporting Information

ABSTRACT: The photoactive yellow protein (PYP) from *Halorhodospira halophila* (Hhal) is a bacterial photoreceptor and model system for exploring functional protein dynamics. We report ultrafast spectroscopy experiments that probe photocycle initiation dynamics in the PYP domain from the multidomain PYP-phytochrome-related photoreceptor from *Rhodospirillum centenum* (Rcen). As with Hhal PYP, Rcen PYP exhibits similar excited-state dynamics; in contrast, Rcen PYP exhibits altered photoproduct ground-state dynamics in which the primary I_0 intermediate as observed in Hhal PYP is absent. This property is attributed to a tighter, more sterically constrained binding pocket around the *p*-coumaric acid chromophore due to a change in the Rcen PYP protein structure that places Phe98 instead of Met100 in contact with the chromophore. Hence, the I_0 state is not a necessary step for the initiation of productive PYP photocycles and the ubiquitously studied Hhal PYP may not be representative of the broader PYP family of photodynamics.

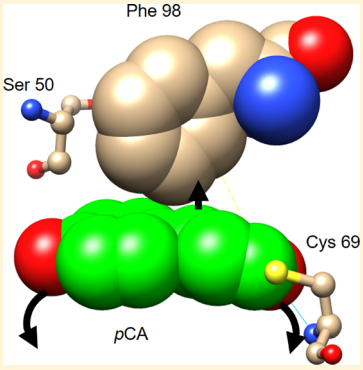

The detection, interpretation, and utilization of sunlight by a wide range of organisms using specialized proteins is the dominant mechanism supporting the Earth's biosphere. While light-induced electron transfer is the primary event during photosynthesis and CO_2 fixation in chlorophyll-based proteins,[1,2] light-induced chromophore isomerization is the primary event for triggering signaling pathways in many photoreceptor families.[3,4] Photoreceptors are critical for the design and production of emerging optogenetic tools.[5] Insights into how the relationship between the protein structure and the chromophore affect the absorption spectra, photodynamics, and quantum yields of photoreceptors provide guidance for improving proteins for emerging optogentic applications.

Multidomain photoreceptors containing a photoactive yellow protein (PYP) module, such as the PYP-phytochrome-related (Ppr) photoreceptor from *Rhodospirillum (R.) centenum*,[6,7] are prime components for these emerging materials as they are responsive to multiple distinct colors of light. Ppr regulates gene expression of chalcone synthase,[6] a key intermediate in the formation of photoprotective pigments, with a three-domain protein consisting of a blue-absorbing PYP[8,9] domain, a red-absorbing bacterial phytochrome (Bph) domain, and a His kinase output domain.[10,11] How the interactions between the PYP and Bph photoreceptor couple to biological activity is unclear, but is clearly cooperative with the photochemistry of the full-length Ppr complex[12,13] differing from the photochemistry of the isolated components. For example, photoexcitation of both domains results in an increased recovery time compared to the excitation of either domain separately.[12] Furthermore, multidomain interactions may create a heterodimer to transform PYP and Bph domains in Ppr from a blue/red light sensor into a UV/red light sensor.[13]

The PYP domain in Ppr (Rcen PYP) resembles the widely studied PYP from *Halorhodospira halophila* (Hhal PYP); the proteins share 45% sequence identity and 60% sequence similarity. The sequences indicate that the *p*CA binding pockets of the two PYPs are largely conserved with the exception of residue 50, a threonine in Hhal PYP and a serine in Rcen PYP (Scheme 1). The X-ray crystal structures of Rcen PYP[14] reveal a difference not predicted by the sequence alone: the β4-β5 loop is positioned such that Phe98 is closest to the *p*-coumaric acid (*p*CA) chromophore, instead of Met100 as is the case in Hhal PYP.[14] Similar to long-living Hhal PYP Met100 mutants,[15] Rcen PYP exhibits a longer photocycle recovery half-life of 46 s[6] compared to 400 ms for Hhal PYP.[16]

The ground-state absorption (GSA) spectrum of Rcen PYP is blue-shifted (Figure 1, red) compared to Hhal PYP (Figure 1, black), with peaks at 435 and 446 nm, respectively. The difference in the absorbance spectrum is likely not due to different spectral inhomogeneities as both PYPs exhibit comparable GSA bandwidths. The origin of the blue-shifted GSA of Rcen PYP is unclear, but is tentatively ascribed to an

Received: September 30, 2016
Accepted: December 2, 2016
Published: December 2, 2016

DOI: 10.1021/acs.jpclett.6b02253
J. Phys. Chem. Lett. 2016, 7, 5212−5218

Scheme 1. Important Protein Residues around the Chromophore Pockets of Hhal PYP[17] (right, PDB 2PYP) and Rcen PYP[14] (left, PDB 1MZU)[a]

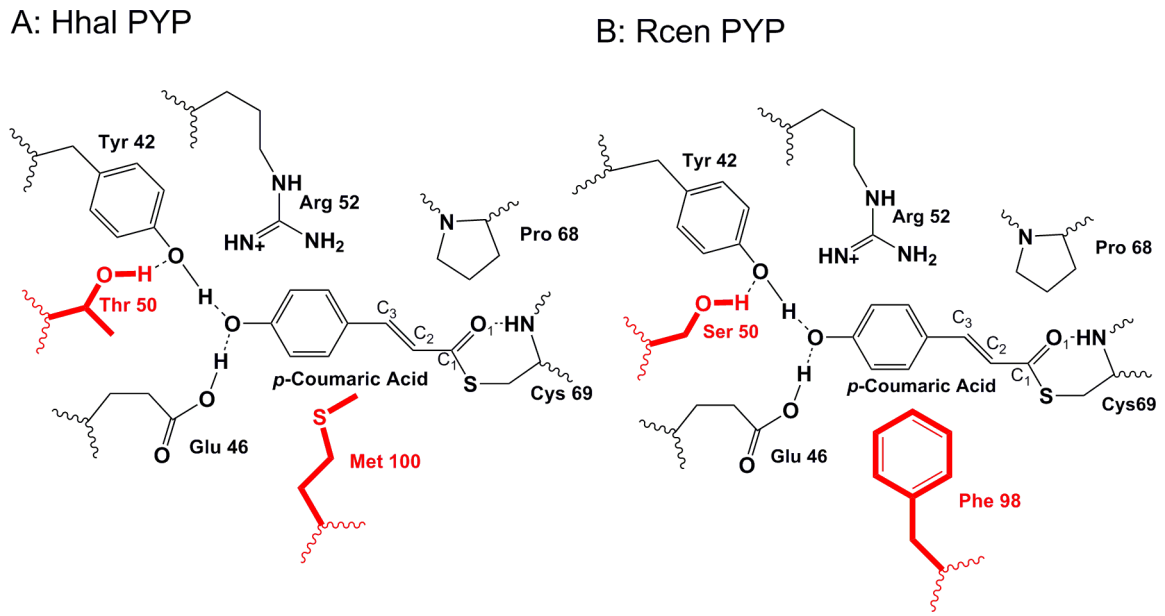

[a]Residues in red are different between the two proteins. Relevant atoms in the *p*CA chromophore are labeled.

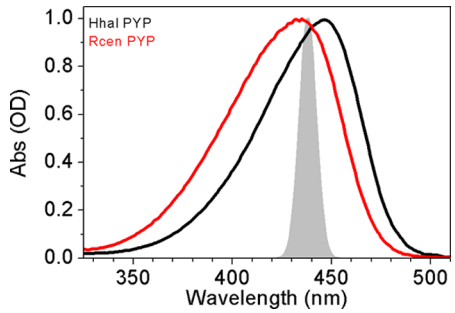

Figure 1. Static absorption spectra for Rcen PYP (red curve) compared to the spectrum of Hhal PYP (black curve). The laser spectrum of the 438 nm excitation pulses (filled gray curve) is overlapped.

increase in hydrogen bonding between the proteins and the phenolic group of the embedded *p*CA chromophore (Scheme 1). Comparative studies of Hhal PYP mutants have identified that decreasing the strength of hydrogen bonding to *p*CA induces a greater charge density on the phenolic group and results in red-shifted GSA spectra.[18−20] However, the crystallographic structure of Rcen PYP revealed no substantial differences in the hydrogen bonding networks of the two PYPs.[14] Subtle changes in active site hydrogen bonding that alter electronic GSA may not be resolved with the 2.0 Å resolution of the structure of Rcen PYP.

The transient absorption (TA) spectra of Rcen PYP from −10 ps to 7 ns in the spectral region of 350−660 nm were measured and contrasted to the corresponding transient signals in Hhal PYP[21] (Figure 2). The signals of both samples were measured consecutively on the same experimental setup and under the same experimental conditions (given in the Supporting Information) to allow direct comparison of the data. The 438 nm excitation wavelength was selected to avoid multiphoton ionization of *p*CA.[22,23] While the GSA spectra differed slightly between the two proteins, the excited-state pG* spectrum of Rcen PYP (Figure 2A) is nearly identical to that of Hhal PYP (Figures 2C and S1). Both proteins exhibit broad excited-state absorption (ESA) bands peaking at 375 nm, ground-state bleaches (GSBs) at around 440 nm, and stimulated emission (SE) bands peaking at 500 nm. The nearly identical pG* spectra indicate that the proteins share comparable vibrationally relaxed *p*CA structures on the excited-state surfaces, irrespective of the protein interactions responsible for the differing GSA spectra (Figure 1).

The excited-state quenching kinetics of pG* are reflected in the ESA and SE traces at 375 and 500 nm, respectively (Figure 3A). For Rcen PYP, these dynamics are similar, albeit slightly slower, to Hhal PYP (Figure 3C), with a ∼2 ps half-life for the overall amplitude of the signal and complete decay within 100 ps. While the excited-state dynamics of pG* for both proteins are comparable, the subsequent ground-state photoproduct dynamics (>10 ps) differ significantly. Within the 7 ns time scale of the experiment, Hhal PYP exhibits the well-resolved I_0 photostate peaking at 500 nm (Figure 2D, blue curve) that evolves into the pR photostate at 480 nm (black curve).[22] The evolution of I_0 into pR is resolved in nonmonotonic kinetics with a decay of the 500 nm trace (Figure 3D, red curve) coupled with the rise of the 475 nm trace (Figure 3D, green curve) at nanosecond time scales.

In contrast, the 500 and 475 nm kinetics of Rcen PYP (Figure 3B, red and green curves) exhibit differing dynamics, with the 475 nm trace always more positive than the 500 nm trace. Despite these differing kinetics, the spectrum of Rcen PYP (Figure 2B, blue curve) is similar to the terminal spectrum of Hhal PYP (Figure 2D, black curve).

The transient data sets were analyzed with a multicompartment global analysis formalism[24,25] that decomposes the data via a postulated model into *time-dependent* populations (i.e., concentration profiles) with *time-independent* spectra. If the underlying target model accurately describes the dynamics, the extracted spectra from the analysis are termed species associated difference spectra (SADS) and represent the

DOI: 10.1021/acs.jpclett.6b02253
J. Phys. Chem. Lett. 2016, 7, 5212−5218

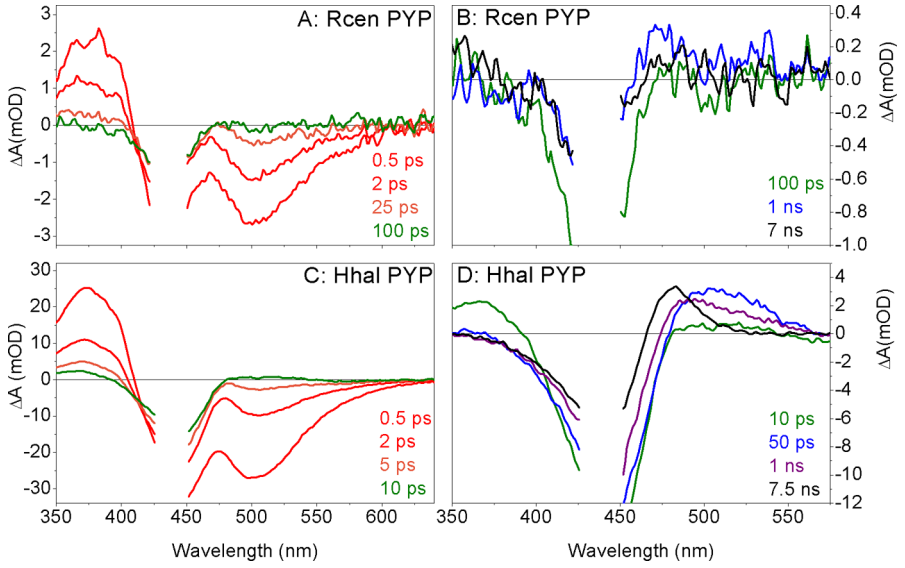

Figure 2. TA spectra at selected times from Rcen PYP (A,B) compared to Hhal PYP transient spectra from a previous study (C,D). The data perturbed by the scattering of the 438 nm excitation light have been excised from the spectra. The smaller amplitude of the Rcen PYP signals is attributed to the sample's 10-fold reduced concentration.

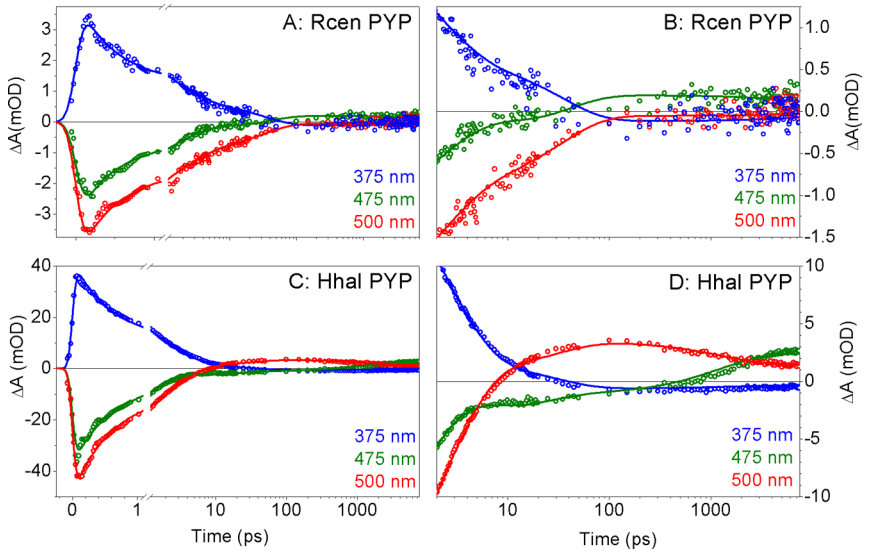

Figure 3. Kinetic traces at selected wavelengths for the TA spectra shown in Figure 2 for Rcen PYP (top row) and Hhal PYP (bottom row). The solid curves are fits of the data to the respective models in Figure 4.

difference spectra of the constituent transient populations. For both PYP samples, a triphasic heterogeneous model was adopted based on previous analysis of Hhal PYP (Figure 4A,B).[19,21,22,26] Within these models, the observed nonexponential quenching kinetics is attributed to the dynamics of three independently photogenerated pG* populations that either decay directly back into the ground-state pG populations, relax into a transiently lived ground-state intermediate (GSI), or initiate the photocycle.

For Rcen PYP, excitation of the three pG populations generates three independent pG* populations (with 50, 40, and 10% occupancies) with apparent (i.e., experimentally observed) decay time constants of 0.5, 3.9, and 45 ps (Figure 4A and Table S1). The corresponding decay constants of the pG* populations in Hhal PYP are surprisingly similar to 0.5, 2.7, and 45 ps and occupancies of 52, 42, 6%, respectively (Figure 4B). The close agreement between Hhal PYP and Rcen PYP pG* decay kinetics reflects the similar protein environment around *p*CA (Scheme 1) and the similarity of the pG* spectra (Figure S1).[6,14] The short-lived GSI populations are for highly excited vibrational *p*CA in the electronic ground state and are observed in both Rcen PYP (Figure 4C, blue curve) and Hhal PYP (Figure 4D, blue curve). The GSI in Rcen PYP is slightly blue-shifted compared to that in Hhal PYP,[22] but this likely is the result of its blue-shifted GSA spectrum (Figure 1).

The primary photoproduct I_0 in the photocycle of Hhal PYP (Figure 4C, green) is not observed in the raw spectra of Rcen PYP. If a short-lived I_0 population were to exist in Rcen PYP, as we recently observed in the PYP from *Leptospira biflexa* (Lbif PYP),[21] then differing decay kinetics of SE and ESA bands would be present. In Lbif PYP, the differing kinetics were interpreted through global analysis as caused by a short-lived (2.4 ps lifetime), but resolvable, I_0 population that coexists with appreciably longer lived pG* populations (~100 ps lifetime).[21]

DOI: 10.1021/acs.jpclett.6b02253
J. Phys. Chem. Lett. 2016, 7, 5212−5218

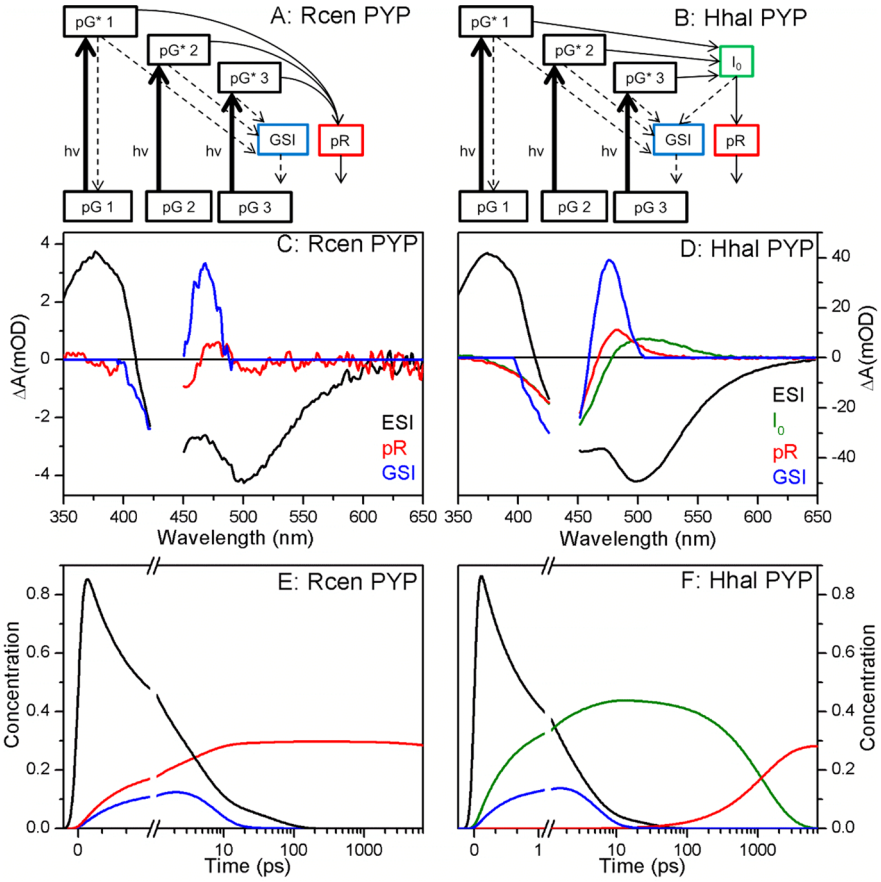

Figure 4. Global analysis of the ultrafast spectroscopy data for Rcen PYP (left column) and Hhal PYP (right column). (A,B) Target models. (C,D) Species SADS extracted from global analysis. (E,F) Concentration profiles. The quality of global analysis fits of these models to the respective data is depicted in Figure 3.

As differing kinetics are not observed in Rcen PYP after the initial 200 fs signal rise time, for a similar hidden fast I_0 population to exist, it would need to have a lifetime less than the 200 fs instrument response function. A hypothetical I_0 with a <200 fs lifetime is considerably faster than any known photoproduct in PYP. For these reasons, I_0 was excluded in the global model for Rcen PYP and presumed absent from the resulting photocycle. Alternatively, if I_0 were to be slowly generated but then rapidly decay, it also would not be observed in the data. Neither fast nor slow I_0 generation hypotheses can be introduced into our global analysis because they generate unseen populations and are technically possible. The premise of our arguments is that the absence of I_0 signals in our transient data is a signature of the absence of the I_0, and while this approach follows an Occam's razor perspective, it does not exclude other hypotheses with exceedingly fast sub-200 fs lifetimes.

The primary photoproduct in Rcen PYP (Figure 4A, red curve) strongly resembles pR in Hhal PYP (Figure 4C, red curve). The SADS for the Rcen PYP pR spectrum is slightly blue-shifted relative to that for the Hhal PYP pR spectrum, which agrees with the blue-shifted GSA (and hence GSB) of Rcen PYP (Figure 1). A weak positive feature at around 375 nm is resolved in the primary photoproduct of Rcen, which is reminiscent of the pUV state recently identified in Lbif PYP.[21,27]

The quantum yield of the formation of pR in Rcen PYP is estimated at 30 ± 5% from the global analysis. In this estimation, we assume that the relative extinction coefficients for the ESA and the GSI are comparable in Rcen PYP and Hhal PYP, and the ratio of the GSI amplitude to the pG* ESA amplitude should be equal (Figure S1). Therefore, any changes to the absorbance reflect changes in the populations of the SADS and the yield of the pR intermediate. The pR yield in Rcen PYP derived through this analysis is similar to that obtained for pR in Hhal PYP at 29 ± 3%. However, the latter case pR is a secondary photoproduct formed through thermal decay of the I_0 primary photoproduct. In Hhal PYP, the primary I_0 state is produced with a 45% yield, higher than the 30% yield of the primary Rcen PYP pR product, and 64% of the Hhal PYP I_0 state proceeds to pR. Rcen PYP bypasses I_0 but generates pR with a (probably coincidentally) comparable yield.

One possible explanation for the absence of an I_0 intermediate in Rcen PYP is weaker hydrogen bonding by the Ser50 residue. Of the 140 known members of the PYP family, only 15 proteins contain Thr50 (e.g., Hhal PYP) and another 31 proteins used Ser50 (e.g., Rcen PYP); Ala50 is also commonly observed at this position (e.g., Lbif PYP).[9] Hence, position 50 is the least conserved of the active site residues and therefore might be the least critical residue for achieving productive protein photodynamics.[9] In the case where weak hydrogen bonding from Ser50 is influential, the ultrafast photocycle dynamics of Rcen PYP would be expected to resemble that of mutants in which the hydrogen bond to *p*CA from residue 50 is absent. In the Hhal PYP T50V mutant,[19] and wild-type Lbif PYP,[21] the absence of a hydrogen bond between

DOI: 10.1021/acs.jpclett.6b02253
J. Phys. Chem. Lett. 2016, 7, 5212−5218

residue 50 and Tyr42 significantly slows the excited-state dynamics by shifting population into pG* states with longer lifetimes. Neither Hhal PYP T50V nor Lbif PYP decreases the photocycle initiation quantum yield or eliminates the I_0 state. However, Rcen PYP does not follow these trends; it exhibits fast excited-state dynamics, a similar quantum yield of pR formation compared to Hhal PYP (30% versus 29%), but with no visible I_0 population. We conclude that the Thr50 to Ser50 difference in Rcen PYP is unlikely to be responsible for the observed absence of the I_0 intermediate.

A more plausible explanation for the differing photocycle initiation dynamics for Rcen PYP and Hhal PYP is ascribed to the structural changes in the Met100 region of the protein. Although both proteins have Met at position 100, the crystal structure of Rcen PYP[14] indicates that the shape of the $\beta4-\beta5$ loop is altered. As a result, while in Hhal PYP the Met100 side chain is positioned immediately above the *p*CA chromophore, in Rcen PYP, the bulkier Phe98 side chain occupies this location in Rcen PYP (Schemes 1 and 2). In the Hhal PYP pG

Scheme 2. Chromophore Binding Pocket of Hhal PYP[17] (A, PDB 2PYP) and Rcen PYP[14] (B, PDB 1MZU) with Space-Filling Models to Emphasize the Congestion in the Pocket Caused by the Structural Differences[a]

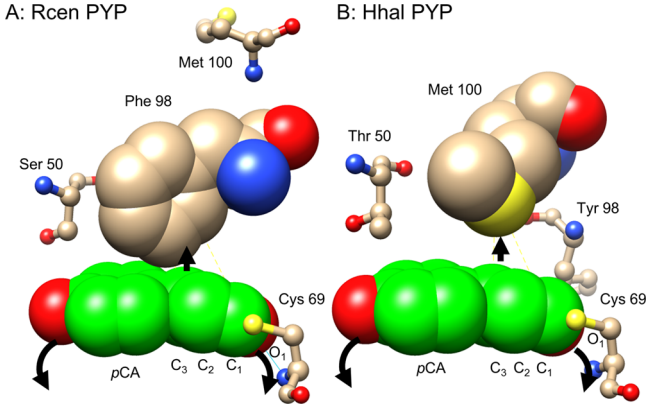

[a]Arrows indicate the direction of movement during formation of the I_0 state in Hhal PYP.

structure,[28] the distance between the Met100 sulfur and C3 of *p*CA is 4.6 Å, while the distance between the Phe98 ring and C3 *p*CA in the Rcen PYP pG structure[14] is closer at 3.6 Å (Table S2).

The time-resolved X-ray crystallographic studies of Hhal PYP by Ihee et al.[29] and Schotte et al.[30] both show that the I_0 (labeled I_T and pR_0 in their studies, respectively) results from the thioester oxygen (O1) of the *p*CA swinging out of plane of the *p*CA phenolate moiety (Scheme 2). This single bond rotation quenches pG*, puckering the molecule in a strained C-shape, pushing the C2 and C3 carbons up toward the Met100 and the phenolate head down (Scheme 3). In Hhal PYP, the puckered I_0 state is followed by a second single bond rotation[30] to relieve the strain and generate the more planar *cis*-*p*CA in the pR configuration (Scheme 3). Ihee et al. further argued that the photocycle bifurcates after I_0, which agrees with cryokinetics experiments[31] and ultrafast measurements of Lbif PYP[21] (omitted from Scheme 3 for clarity). In the case of Rcen PYP, the space required for the *p*CA chromophore to twist and pucker into the strained I_0 configuration is occupied by the much bulkier Phe98 residue (Scheme 2). We postulate that

Scheme 3. Schematic Depiction of the Rcen and Hhal PYP Photocycles[a]

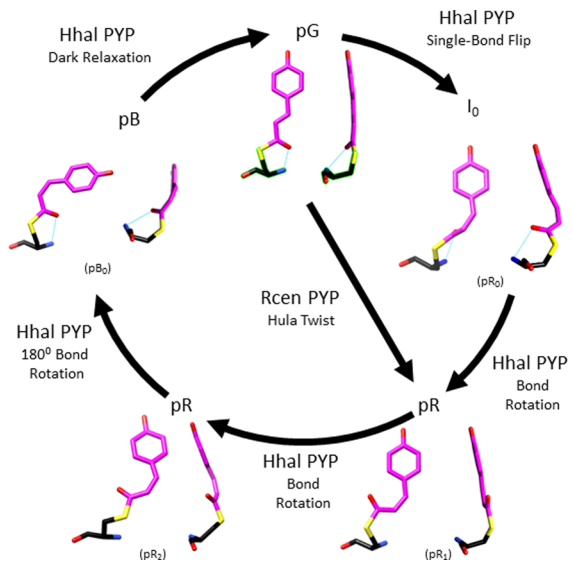

[a]Top views are on the left and side views are on the right of the pCA chromophore (magenta) for each state. Met100 or Phe98 residues are positioned above the *p*CA out of the plane of the paper in the top view and to the right of the *p*CA in the side view. The pG structure was obtained from PDB 2PYP[17] and I_0, pR (pR_1), pR_2, and pB were obtained from PDB 4B9O, 4BBT, 4BBU, and 4BBV, respectively.[30]

Phe98 hinders I_0 formation via a single bond flip to favor the direct formation of the *cis*–*p*CA pR (pR_2 in Schotte et al.[30]) via a more volume conserving hula twist[32] isomerization mechanism (Scheme 3). In this proposal, the repositioning of Phe98 and Met100 in the *p*CA binding pocket of Rcen PYP modifies the photocycle so that pG* is quenched by a hula twist motion, skipping I_0 and directly producing pR with similar kinetics, and yields to the two-step process in Hhal PYP. Both proteins then proceed to generate the signaling pB (Scheme 3) state that then relaxes back to pG on a 38 s and 400 ms time scale for Rcen and Hhal PYP, respectively. These considerations indicate that the initiating and propagation of the PYP photocycle does not require evolution through the I_0 state. The mechanistic importance of the I_0 state in the PYP family may have been overstated based on considering only the dynamics of Hhal PYP.

To conclude, we have measured the ultrafast dynamics of the PYP domain from the Ppr protein of *Rhodospirillum centenum* and compared that to the PYP from *Halorhodopsira halophila.* In both the raw data and global analysis, the pG* dynamics are comparable in Rcen PYP and Hhal PYP. However, the proteins diverge in the photocycle initiation dynamics, with I_0 not being populated in Rcen PYP and populated in Hhal PYP. On the basis of previous knowledge of the mechanism of *p*CA photoisomerization and the crystal structures of these two photoreceptors, we demonstrate that the I_0 state is not a necessary step for the initiation of productive PYP photocycles and may not be a general state ascribed to the PYP family of photoreceptors. We attribute deviations of Rcen PYP from the case of Hhal PYP to the altered placement of the large side chain of Phe98 in the chromophore pocket of the ground state of Rcen PYP. The pR quantum yield for both systems is comparable at 30%. Rcen PYP joins Hhal and Lbif as the only non-Hhal PYPs that have had the primary dynamics

DOI: 10.1021/acs.jpclett.6b02253
J. Phys. Chem. Lett. 2016, 7, 5212–5218

characterized. Of these three proteins, Rcen PYP is unique in that no I_0 population is observed. These data indicate that the dynamics of the ubiquitously studied Hhal PYP may not be representative of the photodynamics of the broader PYP family.

■ ASSOCIATED CONTENT

Supporting Information

The Supporting Information is available free of charge on the ACS Publications website at DOI: 10.1021/acs.jpclett.6b02253.

DNA primer sequences, experimental setup diagrams, global analysis parameters, and addition figures showing normalized species associated difference spectra (PDF)

■ AUTHOR INFORMATION

Corresponding Author

*E-mail: dlarsen@ucdavis.edu.

ORCID

Delmar S. Larsen: 0000-0003-4522-2689

Present Address

§M.K.: Science Department, Sanshinkinzoku, Co. Ltd., 2-5-20 Niihama, Tadaoka-cho, Senboku-gun, Osaka 595-0814, Japan.

Notes

The authors declare no competing financial interest.

■ ACKNOWLEDGMENTS

This work was supported by a grant from the National Science Foundation (CHE-1413739) to D.S.L. and W.D.H. W.D.H. acknowledges additional support from NSF Grants MCB-1051590 and MRI-1338097. Dr. Mikas Vengris (Light Conversion Ltd.) is acknowledged for the donation of global and target analysis software package.

■ REFERENCES

(1) Whitmarsh, J.; Govindjee, Photosynthesis. In *Encyclopedia of Applied Physics*; VCH Publishers Inc., 1995; Vol. *13*, pp 513−532.

(2) Moser, C. C.; Keske, J. M.; Warncke, K.; Farid, R. S.; Dutton, P. L. Nature of Biological Electron Transfer. *Nature* **1992**, *355*, 796−802.

(3) Quail, P. H. Phytochrome: A Light-Activated Molecular Switch That Regulates Plant Gene Expression. *Annu. Rev. Genet.* **1991**, *25*, 389−409.

(4) Bhaya, D. Light Matters: Phototaxis and Signal Transduction in Unicellular Cyanobacteria. *Mol. Microbiol.* **2004**, *53*, 745−754.

(5) Müller, K.; Weber, W. Optogenetic Tools for Mammalian Systems. *Mol. BioSyst.* **2013**, *9*, 596−608.

(6) Jiang, Z.; Swem, L. R.; Rushing, B. G.; Devanathan, S.; Tollin, G.; Bauer, C. E. Bacterial Photoreceptor with Similarity to Photoactive Yellow Protein and Plant Phytochromes. *Science* **1999**, *285*, 406−409.

(7) Kyndt, J. A.; Meyer, T. E.; Cusanovich, M. A. Photoactive Yellow Protein, Bacteriophytochrome, and Sensory Rhodopsin in Purple Phototrophic Bacteria. *Photochemical & Photobiological Sciences* **2004**, *3*, 519−530.

(8) Meyer, T. E. Isolation and Characterization of Soluble Cytochromes, Ferredoxins and Other Chromophoric Proteins from the Halophilic Phototrophic Bacterium Ectothiorhodospira Halophila. *Biochim. Biophys. Acta, Bioenerg.* **1985**, *806*, 175−183.

(9) Meyer, T. E.; Kyndt, J. A.; Memmi, S.; Moser, T.; Colon-Acevedo, B.; Devreese, B.; Van Beeumen, J. J. The Growing Family of Photoactive Yellow Proteins and Their Presumed Functional Roles. *Photochemical & Photobiological Sciences* **2012**, *11*, 1495−1514.

(10) Yeh, K.-C.; Wu, S.-H.; Murphy, J. T.; Lagarias, J. C. A Cyanobacterial Phytochrome Two-Component Light Sensory System. *Science* **1997**, *277*, 1505−1508.

(11) Hughes, J.; Lamparter, T.; Mittmann, F.; Hartmann, E.; Gartner, W.; Wilde, A.; Borner, T. A Prokaryotic Phytochrome. *Nature* **1997**, *386*, 663−663.

(12) Kyndt, J. A.; Fitch, J. C.; Meyer, T. E.; Cusanovich, M. A. The Photoactivated Pyp Domain of Rhodospirillum Centenum Ppr Accelerates the Recovery of the Bacteriophytochrome Domain after White Light Illumination. *Biochemistry* **2007**, *46*, 8256−8262.

(13) Kyndt, J. A.; Fitch, J. C.; Seibeck, S.; Borucki, B.; Heyn, M. P.; Meyer, T. E.; Cusanovich, M. A. Regulation of the Ppr Histidine Kinase by Light-Induced Interactions between Its Photoactive Yellow Protein and Bacteriophytochrome Domains. *Biochemistry* **2010**, *49*, 1744−1754.

(14) Rajagopal, S.; Moffat, K. Crystal Structure of a Photoactive Yellow Protein from a Sensor Histidine Kinase: Conformational Variability and Signal Transduction. *Proc. Natl. Acad. Sci. U. S. A.* **2003**, *100*, 1649−1654.

(15) Devanathan, S.; Genick, U. K.; Canestrelli, I. L.; Meyer, T. E.; Cusanovich, M. A.; Getzoff, E. D.; Tollin, G. New Insights into the Photocycle of Ectothiorhodospira Halophila Photoactive Yellow Protein: Photorecovery of the Long-Lived Photobleached Intermediate in the Met100ala Mutant. *Biochemistry* **1998**, *37*, 11563−11568.

(16) Meyer, T. E.; Yakali, E.; Cusanovich, M. A.; Tollin, G. Properties of a Water-Soluble, Yellow Protein Isolated from a Halophilic Phototrophic Bacterium That Has Photochemical Activity Analogous to Sensory Rhodopsin. *Biochemistry* **1987**, *26*, 418−423.

(17) Genick, U. K.; et al. Structure of a Protein Photocycle Intermediate by Millisecond Time-Resolved Crystallography. *Science* **1997**, *275*, 1471−1475.

(18) Philip, A. F.; Eisenman, K. T.; Papadantonakis, G. A.; Hoff, W. D. Functional Tuning of Photoactive Yellow Protein by Active Site Residue 46. *Biochemistry* **2008**, *47*, 13800−13810.

(19) Changenet-Barret, P.; Plaza, P.; Martin, M. M.; Chosrowjan, H.; Taniguchi, S.; Mataga, N.; Imamoto, Y.; Kataoka, M. Structural Effects on the Ultrafast Photoisomerization of Photoactive Yellow Protein. Transient Absorption Spectroscopy of Two Point Mutants†. *J. Phys. Chem. C* **2009**, *113*, 11605−11613.

(20) Brudler, R.; Meyer, T. E.; Genick, U. K.; Devanathan, S.; Woo, T. T.; Millar, D. P.; Gerwert, K.; Cusanovich, M. A.; Tollin, G.; Getzoff, E. D. Coupling of Hydrogen Bonding to Chromophore Conformation and Function in Photoactive Yellow Protein. *Biochemistry* **2000**, *39*, 13478−13486.

(21) Mix, L. T.; Kirpich, J.; Kumauchi, M.; Ren, J.; Vengris, M.; Hoff, W. D.; Larsen, D. S. Bifurcation in the Ultrafast Dynamics of the Photoactive Yellow Proteins from Leptospira Biflexa and Halorhodospira Halophila. *Biochemistry* **2016**, *55*, 6138−6149.

(22) Larsen, D. S.; van Stokkum, I. H. M.; Vengris, M.; van der Horst, M. A.; de Weerd, F. L.; Hellingwerf, K. J.; van Grondelle, R. Incoherent Manipulation of the Photoactive Yellow Protein Photocycle with Dispersed Pump-Dump-Probe Spectroscopy. *Biophys. J.* **2004**, *87*, 1858−1872.

(23) Larsen, D. S.; Vengris, M.; van Stokkum, I. H. M.; van der Horst, M. A.; de Weerd, F. L.; Hellingwerf, K. J.; van Grondelle, R. Photoisomerization and Photoionization of the Photoactive Yellow Protein Chromophore in Solution. *Biophys. J.* **2004**, *86*, 2538−2550.

(24) van Stokkum, I. H. M.; Larsen, D. S.; van Grondelle, R. Global and Target Analysis of Time-Resolved Spectra. *Biochim. Biophys. Acta, Bioenerg.* **2004**, *1657*, 82−104.

(25) Holzwarth, A. R., Data Analysis of Time-Resolved Measurements. In *Biophysical Techniques in Photosynthesis*; Amesz, J., Hoff, A. J., Eds.; Springer: The Netherlands, 1996; pp 75−92.

(26) Rupenyan, A. B.; Vreede, J.; van Stokkum, I. H. M.; Hospes, M.; Kennis, J. T. M.; Hellingwerf, K. J.; Groot, M. L. Proline 68 Enhances Photoisomerization Yield in Photoactive Yellow Protein. *J. Phys. Chem. B* **2011**, *115*, 6668−6677.

(27) Imamoto, Y.; Shirahige, Y.; Tokunaga, F.; Kinoshita, T.; Yoshihara, K.; Kataoka, M. Low-Temperature Fourier Transform Infrared Spectroscopy of Photoactive Yellow Protein. *Biochemistry* **2001**, *40*, 8997−9004.

DOI: 10.1021/acs.jpclett.6b02253
J. Phys. Chem. Lett. 2016, 7, 5212−5218

(28) Borgstahl, G. E. O.; Williams, D. R.; Getzoff, E. D. 1.4. Å Structure of Photoactive Yellow Protein, a Cytosolic Photoreceptor: Unusual Fold, Active Site, and Chromophore. *Biochemistry* **1995**, *34*, 6278−6287.
(29) Jung, Y. O.; Lee, J. H.; Kim, J.; Schmidt, M.; Moffat, K.; Šrajer, V.; Ihee, H. Volume-Conserving Trans-Cis Isomerization Pathways in Photoactive Yellow Protein Visualized by Picosecond X-Ray Crystallography. *Nat. Chem.* **2013**, *5*, 212−220.
(30) Schotte, F.; et al. Watching a Signaling Protein Function in Real Time Via 100-Ps Time-Resolved Laue Crystallography. *Proc. Natl. Acad. Sci. U. S. A.* **2012**, *109*, 19256−19261.
(31) Imamoto, Y.; Kataoka, M.; Tokunaga, F. Photoreaction Cycle of Photoactive Yellow Protein from Ectothiorhodospira Halophila Studied by Low-Temperature Spectroscopy. *Biochemistry* **1996**, *35*, 14047−14053.
(32) Liu, R. S. H.; Hammond, G. S. The Case of Medium-Dependent Dual Mechanisms for Photoisomerization: One-Bond-Flip and Hula-Twist. *Proc. Natl. Acad. Sci. U. S. A.* **2000**, *97*, 11153−11158.

DOI: 10.1021/acs.jpclett.6b02253
J. Phys. Chem. Lett. 2016, 7, 5212−5218